

Bi-Temporal Analysis of Vegetation Index on Land Surface Temperature in Kottayam, Kerala

VIJAYAKUMAR ANITHA¹, MARIMUTHU PRASHANTHI DEVI²
and DURAISAMY PRABHA^{1*}

¹Department of Environmental Sciences, Bharathiar University, Coimbatore, Tamil Nadu, India.

²Department of Environmental Science and Management, Bharathidasan University, Tiruchirapalli, Tamil Nadu, India.

Abstract

The impact of NDVI (Normalized Difference Vegetation Index) on the LST (Land Surface Temperature) as well as on the genesis of surface heat islands in urban areas during two different time periods was assessed in Kottayam district, Kerala, India. Landsat TM, Landsat OLI and TIRS imagery from the years 1988 and 2020 were employed to scrutinize the relationship between NDVI and LST. The area covered under different NDVI classes were quantified. The finding indicated that NDVI of the research region decreased from 0.77 in 1988 to 0.59 in 2020, resulting in an increase in LST_{max} from 34.46 °C in 1988 to 40.63 °C in 2020. Decrease in NDVI resulted in an increase in the high UHI class from 20.83 km² in 1988 to 660.59 km² and from 7.26 km² to 181.35km² in the very high UHI class. An inverse relationship was observed between NDVI and LST, with Pearson coefficients of 0.5737 and 0.5199 for 1988 and 2020, respectively, which indicates that NDVI could serve as a crucial metric for evaluating LST and UHI effects. Future research will explore the effect of seasonal variability in LULCC on LST, day and night time UHI and their impacts on human health and energy consumption.



Article History

Received: 24 May 2023
Accepted: 10 November 2023

Keywords

Land Surface Temperature;
Landsat OLI and TIRS;
Landsat TM;
Normalized Difference
Vegetation Index;
Urban Heat Island.

Introduction


Accelerated urbanization of a particular area is always associated with the cost of the transformation of its original Land Use and Land Cover (LULC) pattern. This results in the natural green spaces

to undergo a considerable transition into artificial impermeable surfaces like concrete, asphalt and metals etc.¹ Escalation of impervious surfaces increases absorption of solar radiation, storage, and reduction of long-wave radiation loss, lower

CONTACT Duraisamy Prabha ✉ prabha.ens@buc.edu.in 📍 Department of Environmental Sciences, Bharathiar University, Coimbatore, Tamil Nadu, India.



© 2023 The Author(s). Published by Enviro Research Publishers.

This is an  Open Access article licensed under a Creative Commons license: Attribution 4.0 International (CC-BY).

Doi: <https://dx.doi.org/10.12944/CWE.18.3.13>

albedo, thereby affecting air humidity and atmospheric temperature.² All these factors form major contributors for increased Land Surface Temperature (LST) and for the creation of Urban Heat Island (UHI).^{3,4} Green cover provides shade, thus lowering surface temperature thereby reducing surface temperature through evapotranspiration process. But, LULC modification mediated through urbanization reduces green cover, thereby altering the energy balance, thus rendering certain areas warmer than their surroundings, triggering the formation of UHI.⁵

UHI studies can be performed either by measuring air temperature or by measuring the LST.⁶ LST is a response of different types of land covers. Therefore, investigating variations in LST is useful for comprehending the sustainability and ecological health of urban areas. Remote sensing (RS) sensors have the excellent potential to measure LST, and therefore, their successful adoption in UHI studies. Understanding the pattern and intensity of UHI requires an understanding of the differences in surface temperatures of land areas between well-established towns and areas with sparse development or rural settings. As a result, LST turns out to be a critical indicator to detect the level and strength of UHI.^{7,8} Various vegetation indices are also generated employing remote sensing technology to assess vegetation cover. NDVI (Normalized Difference Vegetation Index) is one such index, which is an indicator of LULC change (LULCC) and is employed widely for vegetation extraction. NDVI values are suggestive of greenness intensity of vegetation.⁹

Perusal of literature reveals several reports on LULC changes and associated genesis of UHI and corresponding changes in vegetation index by using satellite images. A temporal analysis of NDVI and LST has been conducted to investigate LULC changes in Iberia.¹⁰ Spatial variability in the LST across Delhi, with the highest LST in urban areas has been reported.^{11,12} An increase in LST with land cover (LC) dynamics was observed in Bangalore.¹³ Reports showed contrast between diurnal and various LC indices on LST over Ahmedabad.¹⁴ Independent studies to assess the impact of LULC change for Surat showed that LULCCs had a significant impact on surface temperature.^{15,16} It has been demonstrated that changes in LULC in Pune

have resulted in increased surface temperature and UHI effect.¹⁷⁻¹⁹ The association between land use change, urban expansion and LST for Jaipur and Chennai have been investigated.^{20,21} Significant research is being conducted across the globe on study of Urban Heat Island (UHI) dynamics employing remote sensing indices, particularly utilizing Landsat imagery. The relationship between LST and vegetation for UHI extraction has been demonstrated for Atlanta, Indianapolis, Wuhan, Skopje, Mekelle city, Northern Ethiopia.²²⁻²⁶ Landsat-derived indices such as the Index Based Built-up Index (IBI) has been demonstrated as valuable tools for precise UHI estimation as has been reported in Istanbul.²⁷ A comparative study was conducted on the NDVI and UHI of Delhi and Mumbai, employing thermal satellite data for investigating the accelerated increase in urban heat and its correlation with NDVI.²⁸ The significance of NDVI and NDBI (Normalized Difference Built-up Index) in unravelling effects of SUHI (Surface Urban Heat Island) in Jasi, employing Landsat 8 (L₈) imagery was demonstrated.²⁹ The study unveiled significant spatial heterogeneity, disparities across seasons, and the influence of correlations between LST and NDVI on SUHI dynamics.³⁰ Seasonal discrepancies in RS indices as well as heat islands on urban surfaces has been witnessed along the boundary lines between the rural and urban areas in Dalian, Northeast China.³¹ NDVI and NDBI analysis on SUHI for Bangalore and New Delhi, indicated that NDBI was a better indicator of SUHI intensity than NDVI for both study areas.³² The urbanization in Jaipur had led to changes in LULC with significant increase in surface temperature resulting in significant negative impact on vegetation.³³ The study demonstrated the importance of considering elevation in UHI studies and indicated the potential of using NDVI and Enhanced Vegetation Index (EVI) as reliable UHI indicators. Changes in LULC based on NDVI and Normalized Difference Moisture Index (NDMI) have been reported in Charaideu district of Assam.³⁴ However, there is a paucity of reports on the LULC index and LST and UHI aspects in Kerala, India. The majority of studies in Kerala were reported for Ernakulam and very few research is done on Thiruvananthapuram, Wayanad, and Alappuzha.³⁵⁻³⁸ Reports on NDVI and UHI in Kerala's Kottayam district is inadequate. Therefore, main aspect of the present work was to analyze the potential influence

of NDVI on LST and associated UHI phenomena in Kottayam district from 1988 to 2020, using geospatial techniques.

Data and Methods

Study Location

Kottayam, a central district in Kerala, India is located between 9° 23' 20" and 9° 50' 45" N latitude and 76° 21' 40" and 77° 58' 20" E longitude with an area of 2204 km² and 3 m altitude. It is Kerala's only district that does not border the Arabian Sea or any other state. The district is surrounded by the Idukki district in the east, the Vembanad Lake and Alappuzha district in the west, the Pathanamthitta district in the south and Ernakulam in the North. The Köppen-Geiger classification system categorizes the climate in this region as "Am." (<https://en.climate-data.org/asia/philippines/zambales-1832/>). Kottayam

enjoys a tropical climate with intense hot season in the plains and ample rains throughout the year. The district experiences relatively constant temperatures, averaging between 25°C (77°F) and 32°C (90°F), owing to its proximity to the equator. Following the hot season, which spans from March to May, the southwest monsoon persists from June to September. Gradual increase in daytime temperatures occur throughout the post-monsoon months of October and November, when the heat is almost as intense as in summer. Northeast monsoon is from December to February, and the rainfall ceases in early January. Typically, the region experiences an annual precipitation of 3130.33 millimeters. The district comprises 5 taluks namely, Vaikom, Kottayam, Meenachil, Changanassery and Kanjirappally (Fig. 1).

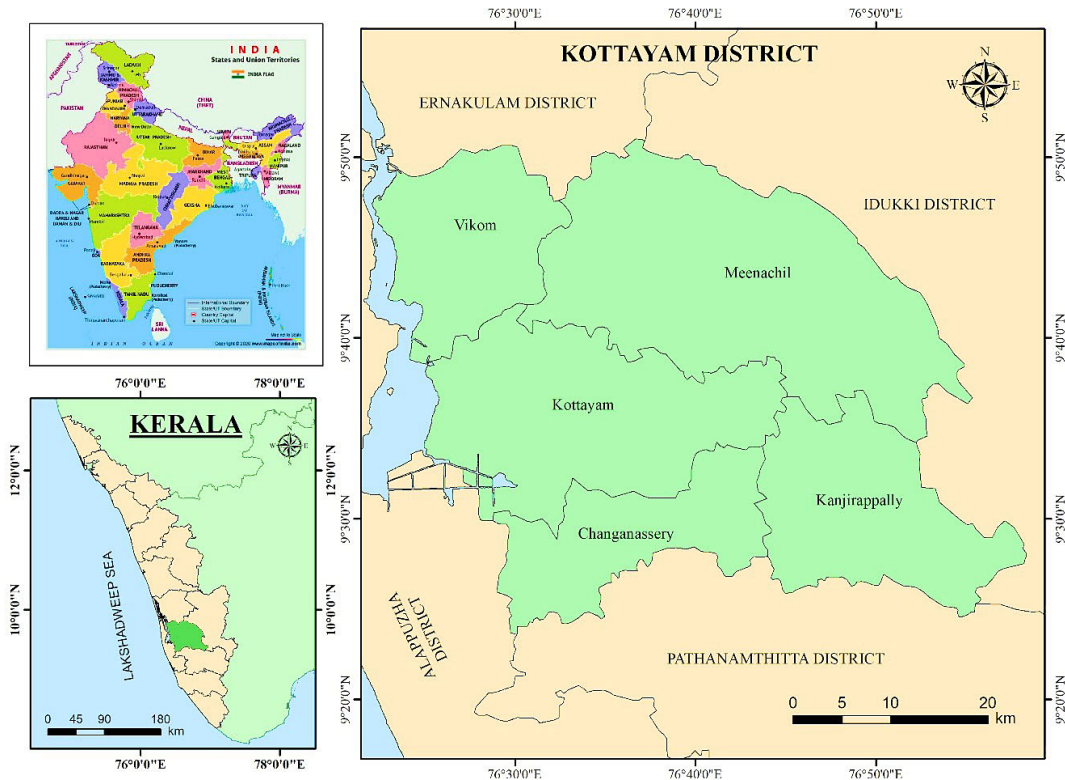


Fig. 1: Map of the study area.

Methodology

Remote Sensing (RS) Data

Landsat images (path/row:144/53) procured from

the website of United States of Geological Survey (USGS) (<https://earthexplorer.usgs.gov/>) over two different periods was used for analysis using

ArcGIS 10.5 software. To minimise atmospheric and seasonal effects, Landsat 5 TM (L5) (1988) and Landsat 8 (L8) OLI/TIRS (2020) with a 30 meter spatial resolution for the same month (January) were used. The two imageries were registered to a common UTM (Universal Transverse Mercator) coordinate system, Zone 43N, with UTM

WGS (World geocoded system) 1984 Projection parameters. ArcGis software was employed for standard image pre-processing techniques like extraction, georeferencing, atmospheric correction, layer stacking, and subsetting. A detailed description of the two Landsat data is presented in Table 1.

Table 1: Details of satellite dataset

Satellite	Sensor	Path/ Row	Date of Image Acquisition	Spatial Resolution	Cloud cover
Landsat-5	Thematic Mapper (TM)	144/53	19/01/1988	30	9%
Landsat-8	Operational Land Imager and Thermal Infrared Sensor (OLI & TIRS)	144/53	27/01/2020	30	7%

Retrieval of LST

Data from a satellite image is shown as Digital Number (DN), indirectly representing the brightness value of ground objects. Thermal bands 6 and 10 respectively for L₅ and L₈ are employed for LST computation. Even though Landsat 8 has two thermal spectral bands, 10 and 11, only 10 is employed in this study's LST computation.^{39,40} Band 11 is not used according to USGS recommendation due to the high calibration uncertainty. However, the extraction process of LST from Landsat TM and Landsat OLI differs slightly in terms of calculating spectral radiance (L_λ).

Conversion of the DN to L_λ

Converting the DN of terrestrial objects to spectral radiance adopting equation 1 in the TIRS sensor is the basic step in LST retrieval.^{39,41} The L_λ from thermal bands of L₅ and L₈ is calculated using the following equation.

For Landsat 5,

$$L_{\lambda} = \frac{(L_{MAX_{\lambda}} - L_{MIN})}{(Q_{calMAX} - Q_{calMIN})} \times (Q_{cal} - Q_{calMIN}) + L_{MIN} \quad \dots(1)$$

In the above equation, L_λ represents Spectral Radiance, L_{MAXλ} corresponds to maximum spectral radiance (15.303 for L₅ and 17.04 for L₈), L_{MIN} signifies for the minimum spectral radiances (1.238 for TM), Q_{calMIN} denotes the minimum DN value (1), Q_{calMAX} designates maximum DN Value (255), QCal represents the DN of band 6.

The values for L_{MIN}, L_{MAX}, QCal_{MIN} and Qcal_{MAX} were acquired from metadata file attached with Landsat images.

For L₈ thermal band, top of atmospheric radiance (L_λ) was computed using the approach described below.⁴²

For Landsat 8,

$$L_{\lambda} = M_L * Q_{cal} + A_L \quad \dots(2)$$

Here, M_L represents band-specific multiplicative rescaling factor (value = 0.0003342), Q_{cal} signifies digital numbers of band 10, A_L stands for the band-specific additive rescaling factor (0.1)

Transformation of L_λ into At-satellite brightness temperature (TB): The equation (3) was employed to deduce At-satellite brightness temperature from spectral radiance.

$$TB = \frac{K_2}{\ln\left[\frac{K_1}{L_{\lambda}} + 1\right]} \quad \dots(3)$$

Where, TB signifies the satellite brightness temperature in Kelvin (K), K₁ and K₂ are calibrated constants specific to the TM and OLI & TIRS Sensors. K₁ and K₂ values for Landsat 5TM were 607.76 and 1260.56 and 666.09 and 1287.71 1321.0789 for Landsat 8 OLI.^{36,39,41}

Kelvin (K) to Celsius (°C) degrees

$$TB = \frac{K_2}{\ln\left[\frac{K_1}{L_\lambda} + 1\right]} - 273.15 \quad \dots(4)$$

LST calculation

The obtained temperature values referred to as black body temperatures were corrected for spectral emissivity (ε) to determine LST. Emissivity correction is done according to the nature of land cover by using NDVI values for every individual pixel.⁴³ The emissivity corrected LST have been computed following,⁴⁴

$$LST = \left[\frac{TB}{1 + (\lambda * TB / \rho) * \ln(\epsilon)} \right] \quad \dots(5)$$

Where, LST in °C (Celsius degrees), λ denotes the wavelength of emitted radiance in meters (11.45 for L₅ (Band 6)) and 10.8 (L₈ (Band 10)).

$$\rho = h * c / s = 1.4388 * 10^{-2} \text{ m K} \quad \dots(6)$$

h stands for Planck’s constant (6.626*10⁻³⁴ J s), s signifies the Boltzmann constant, equal to 1.38 * 10⁻²³ J/K, c represents the velocity of light, which is approximately 2.998*10⁸ m/s.

$$\text{Land surface emissivity } (\epsilon) = 0.004 * P_v + 0.986 \quad \dots(7)$$

Applying the equation in the raster calculator, a correction value of 0.986 corresponds to the equation’s adjustment factor. Where the PV (Proportion of vegetation) can be determined as;

$$P_v = \left(\frac{NDVI - NDVI_{min}}{NDVI_{max} - NDVI_{min}} \right)^2 \quad \dots(8)$$

Generally, the NDVI_{minimum} and NDVI_{maximum} values can be revealed directly in the image. NDVI is calculated as:

$$NDVI = \text{Float (NIR-RED)} / \text{Float (NIR+RED)} \quad \dots(9)$$

For L₅, Float (4-3) / Float (4+3)
 For L₈, Float (5-4) / Float (5+4).

Estimation of NDVI

NDVI, a widely used vegetation index, is a descriptor of vegetation phenology that quantifies the disparity between near-infrared and red reflectance by

summing these two components and dividing them.⁴⁵ NDVI extraction was accomplished with the following procedure.^{46,47} Values of NDVI ranges from -1 to 1. Where negative value denotes water and positive values denotes vegetation. High values indicates dense greenery.

$$NDVI = \text{NIR-Red} / (\text{NIR+Red}) \quad \dots(10)$$

Mapping of Urban Heat Island (UHI): LST range value was used to identify UHI by following Equation 11.⁴⁸

$$UHI = (T - T_{min}) / T_{min} \quad \dots(11)$$

T denotes LST raster value, and T_{min} denotes minimum LST value of the study region.

Mapping of Urban Thermal Field Variance Index (UTFVI): The urban thermal ecology and the thermal comfort of the Kottayam region was defined in terms of UTFVI. The value of the LST is proportional to the amount of heat generated. The environmental impact of Kottayam’s UHI zones was assessed using UTFVI, which was calculated as follows (equation 12).⁴⁹

$$UTFVI = (T_s - T_{mean}) / T_{mean} \quad \dots(12)$$

Where, T_s = LST (°C); and T_{mean} = Mean of the LST (°C).

Association between LST and NDVI: The influence of the NDVI on LST was assessed using Pearson’s Product Moment correlation. The correlation was calculated in ArcGIS and Microsoft Excel software using scatter plot tool.

Results and Discussion

Analysis of LST

Mean LST of Kottayam area was 24.82 °C in 1988, which was elevated by 2.55 °C reaching 27.37 °C in 2020 (Fig. 2). Highest temperature was observed at Meenachil taluk which recorded a maximum of 40. 63°C during 2020, whereas low LST of 33.36 °C was recorded in Changanaserry (Fig. 3). LST was categorised into five classes: (a) very low, (b) low, (c) medium, (d) high, and (e) very high. The spatial distribution of LST for the years 1988 and 2020 is illustrated in Fig. 4. Between the years 1988 and 2020, a major shift was observed in areas categorized under medium LST which surged from 740.91 km² in 1988 to 1968.25 km² in 2020 (Table 2).

The year 2020 also observed inclusion of 0.40 km² area under very high LST class in Meenachil taluk, and 0.07 km² in Kanjirapally taluk, which was not prevalent in 1988 (Table 3). The spatial pattern shows migration of Vaikom, Meenachil and Kottayam districts from low temperature zones in 1988 to medium and high temperature zones in 2020. These variations in LST may be attributed to changes in LULC as the developmental activities progresses in those areas. This ultimately reduces vegetative cover, thereby resulting in increased LST. Meenachil, is known for its rapid development and prosperity due to its well established education system, being well-connected to major cities and towns and with excellent access to basic amenities. It is a hub for small and medium sized enterprises, and also a popular tourist destination known for its scenic beauty, green landscapes, temples and social cohesion. Kanjirapally is also a rapidly developing taluk in Kottayam district. People from Kanjirapally have easy access to various parts of Kerala, facilitated by its well-developed infrastructure which includes a railway station and bus stand. Easy access to basic amenities like electricity, water supply etc. are also significant in this taluk, all of these which attracts human settlement in the area, resulting in increased housing and commercial structures. Table 3 summarises the spatial distribution of LST in taluks of Kottayam district in the years 1988 and 2020. Fig. 4 clearly illustrates that LST was high in urban areas whereas areas with vegetative covers and water bodies recorded lower temperatures.

Quantitative research indicates that rapid expansion of urban and/or built-up areas along with impervious materials such as materials used for construction and other infrastructure developments are key factors for increase in urban temperatures and for the resultant changes in the urban and regional climate.⁵⁰ Maximum area under high LST class was observed in Kottayam taluk. Kottayam, being the district headquarters is known for its developmental activities when compared to other taluks in the district. During the years, it has established a well-developed transport infrastructure, bloom in educational institutions and associated infrastructure like hostels etc., healthcare facilities, commercial activities, and well-established tourist destinations, and all those activities which might have accelerated the constructional activities for infrastructural facilities, thereby increasing the concrete and impervious surfaces, eventually resulting in high LST. Enhanced infrastructure, ease in access to raw materials, concentration of good administrative and entrepreneurial and technical expertise, better transport facilities creates a tendency for industries to cluster in Kottayam, thus accelerating urbanisation.⁵¹ Similar changes in spatial distribution of LST due to urbanisation has been reported for several places like Delhi, with high LST in urbanised areas, South Brazil and for Tianjin, China.^{28,11,52,48} Our results corroborates with the findings in Kerala's Ernakulam district where increase in LST owing to LULC changes was demonstrated. Their results showed an increase in built-up area by 2% and decline in waterbodies and wetlands by 1%.³⁵

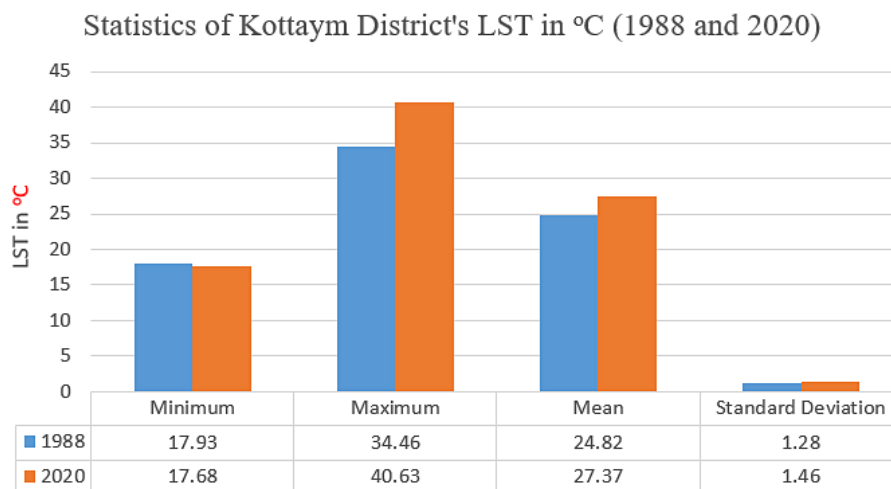


Fig. 2: Statistics of LST (°C) of Kottayam District for the years 1988 and 2020

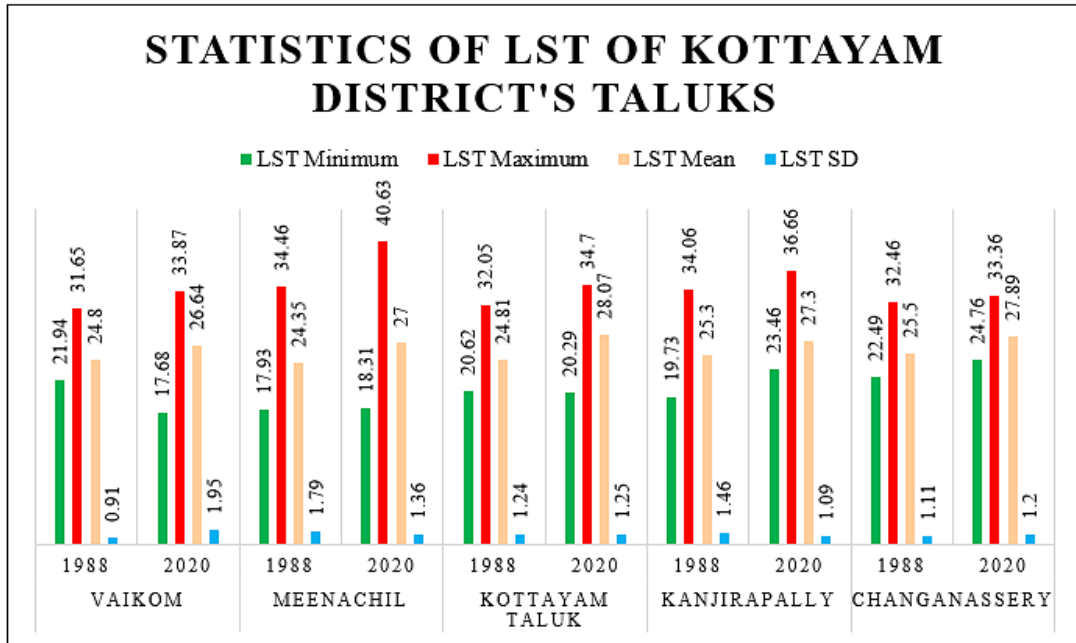


Fig. 3: Taluk wise statistics of LST (°C) of Kottayam District for the years 1988 and 2020

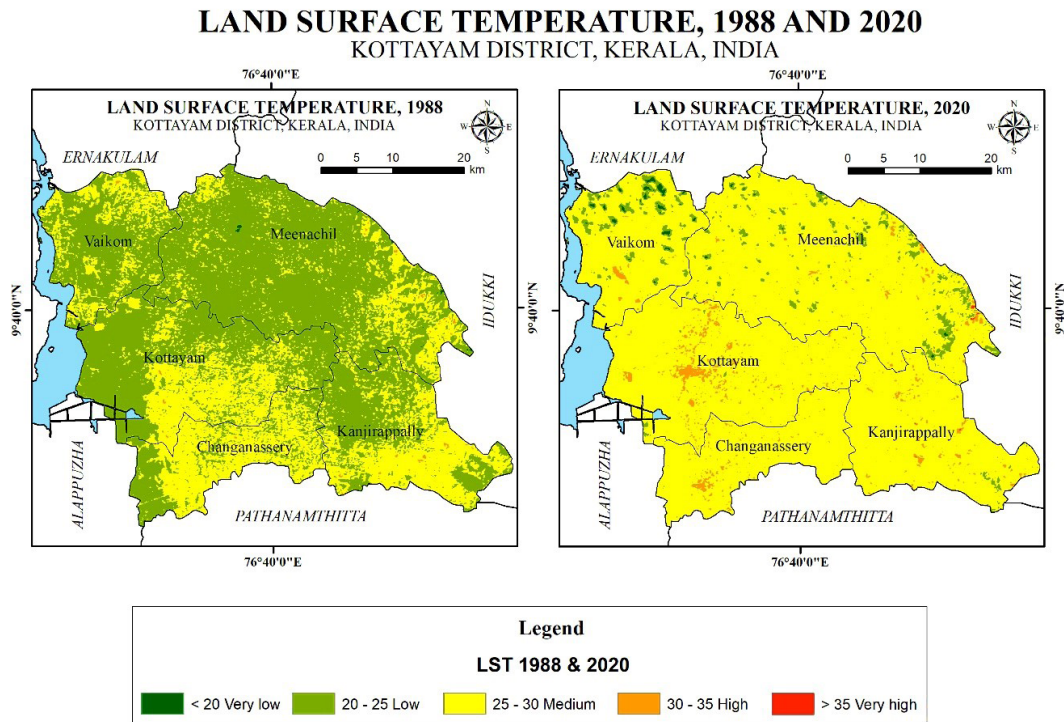


Fig. 4: Spatial distribution of LST (°C) of Kottayam District during 1988 and 2020

Table 2: Spatial distribution of LST (°C) of Kottayam District during 1988 and 2020.

LST (°C) Categories	LST Classes	1988		2020		% Difference (1988 and 2020)
		Area Km ²	Area %	Area Km ²	Area %	
<20	very low	1.05	0.05	6.28	0.30	497.60
20-25	low	1355.84	64.48	75.58	3.59	-94.43
25-30	medium	740.91	35.24	1968.25	93.61	165.65
30-35	high	4.82	0.23	52.04	2.48	979.79
>35	very high	0	0	0.47	0.02	----

Table 3: Taluk wise spatial distribution of LST (°C) of Kottayam district during 1988 and 2020.

LST (°C) Categories	LST Classes	LST Zone in km ²									
		Vaikom		Meenachil		Kottayam		Kanjirappally		Changanassery	
		1988	2020	1988	2020	1988	2020	1988	2020	1988	2020
<20	very low	0	5.21	1.03	1.08	0	0	0.02	0	0	0
20-25	low	188.41	27.10	590.29	44.04	319.95	1.54	169.54	2.78	87.65	0.12
25-30	medium	82.11	235.39	136.60	674.42	177.07	472.03	175.75	336.33	169.39	250.07
30-35	high	0.24	3.06	1.55	9.53	0.83	24.27	1.84	7.97	0.37	7.21
>35	very high	0	0	0	0.40	0	0	0	0.07	0	0

Analysis of NDVI

The NDVI scale is used to evaluate the vegetation status of a particular area. The values of NDVI within the research region ranged from -0.33 to 0.77 in 1988 and -0.14 to 0.59 in 2020 (Fig. 5). Very high vegetation cover was observed at all the taluks in the year 1988, which disappeared in the year 2020. The NDVI values were classified under five groups (Table 4 and Fig. 7): (i) < 0 (no-vegetation); (ii) 0-0.25 (very low); (iii) 0.26-0.45 (sparse); (iv) 0.46-0.59 (moderate); and (v) > 0.60 (highly dense). Major changes were effected in the moderate and highly dense classes. Area under moderate dense class reduced from 61.42% in 1988 to 10.98% in 2020 and high dense vegetation class which was 8.23% in 1988, was not prevalent in 2020, except for a small area of 0.002 km² in Kanjirappally (Table 5). Eventually, the NDVI recorded a maximum of 0.77 and 0.59 during 1988 and 2020 respectively,

at Kanjirappally taluk (Fig. 6). Maximum NDVI in Kanjirappally taluk may be because of its low population compared to other taluks, which would have reduced the removal of vegetative cover for developmental activities. Map describing changes in NDVI, depicting alterations in vegetation area during 1988 and 2020 is shown in Fig. 7. The results indicate decrease in the vegetative cover of the region. Reduction in green cover results in decreased evaporative cooling, thereby causing a rise in LST.

The State of Forest Report 2019 (Forest Survey of India) denotes that all five taluks in Kottayam district have forest cover. The taluks with the highest forest cover are Kanjirappally and Meenachil. However, NDVI analysis showed reduction in high dense forest covers in both the taluks pushing a fraction of the area under a very high LST class (Table 3). This may be due to the conversion of native forests into agroecological

zones, specifically for rubber plantations, which attract farmers due to its economic importance. Kottayam comes under the core rubber producing zone, with the highest production reported from Kanjirapally taluk.⁵³ Conversion of native forests into monoculture plantations such as rubber

imposes detrimental effects on the temperature and microclimate of that area.^{53,54} Kerala has encountered a massive increase in urban land over the years 1973–2016⁵⁵ with expansion of built-up land by replacing vegetation and agricultural land.⁵⁶

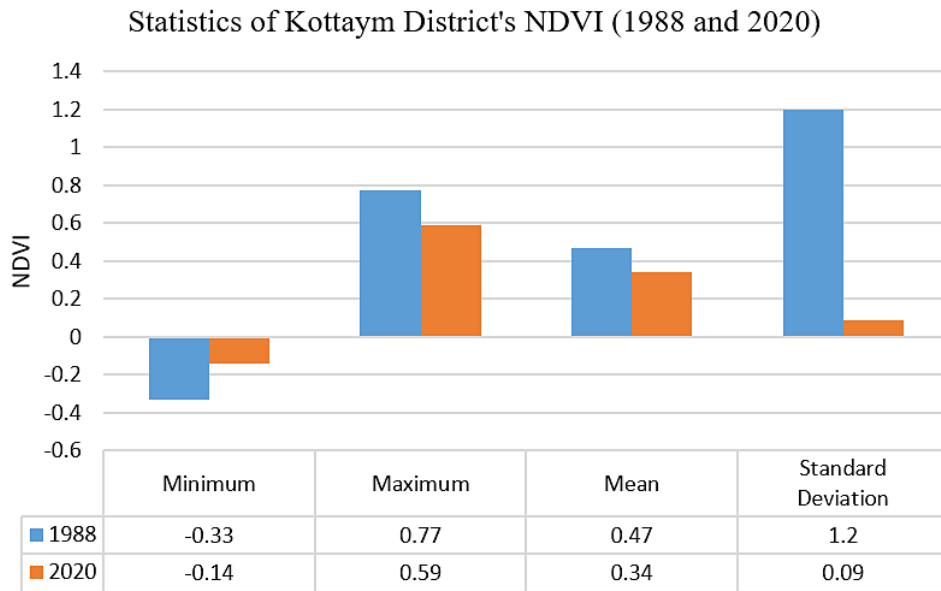


Fig. 5: Statistics of NDVI of Kottayam District during 1988 and 2020

STATISTICS OF NDVI OF KOTTAYAM DISTRICT'S TALUKS

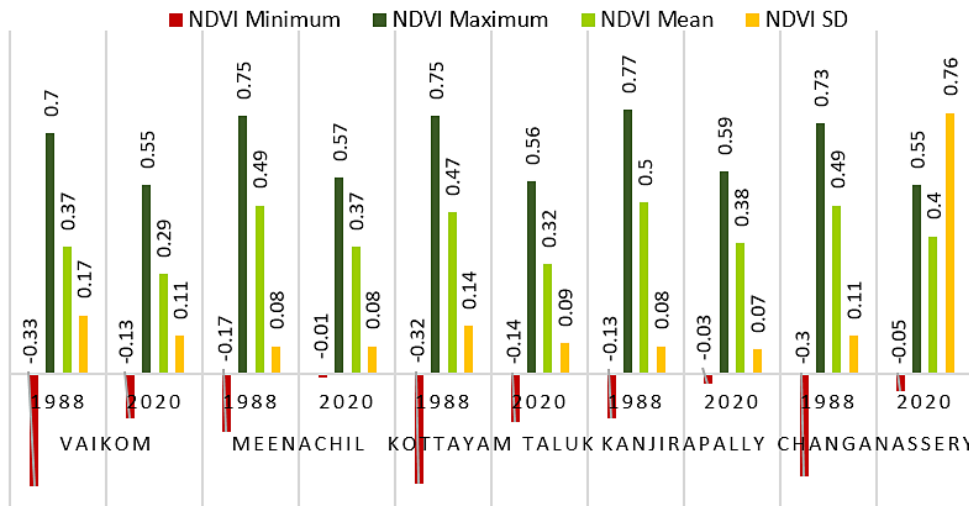


Fig. 6: Taluk wise statistics of NDVI of Kottayam District during 1988 and 2020

NORMALIZED DIFFERENCE VEGETATION INDEX, 1988 AND 2020
 KOTTAYAM DISTRICT, KERALA, INDIA

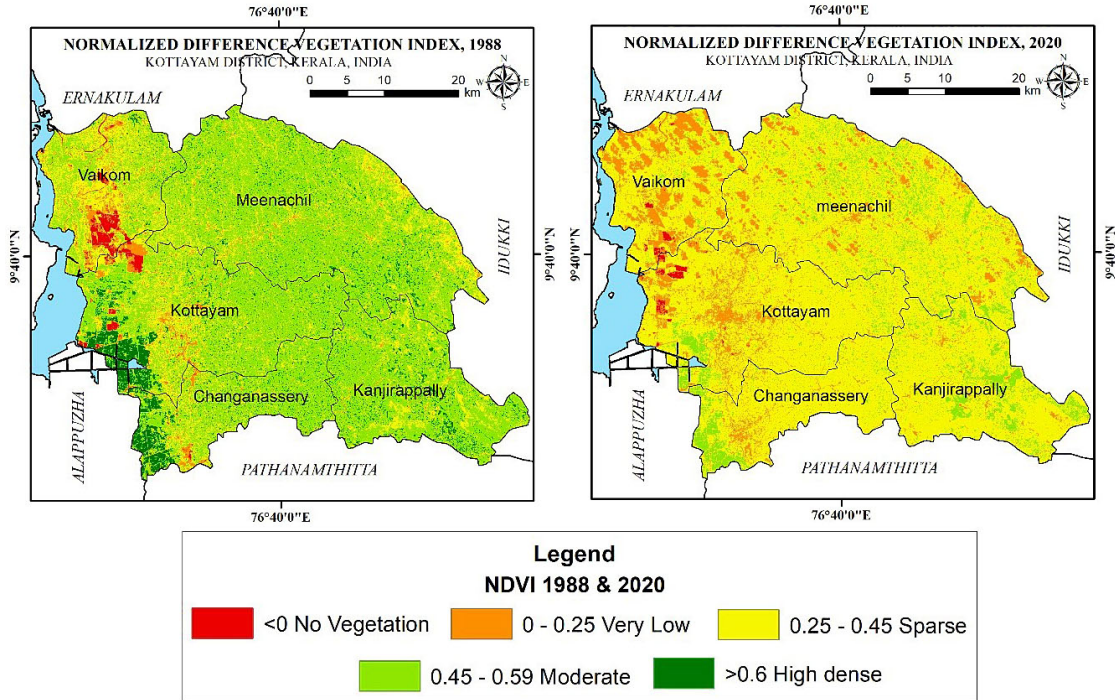


Fig. 7: Spatial distribution of NDVI of Kottayam District for the years 1988 and 2020

Table 4: Spatial distribution of NDVI of Kottayam District during 1988 and 2020.

NDVI Categories	NDVI Classes	1988		2020		% Difference (1988 and 2020)
		Area Km ²	Area %	Area Km ²	Area %	
<0	No Vegetation	25.92	1.23	9.39	0.45	-63.77
0-0.25	Very Low	84.31	4.01	267.85	12.74	217.71
0.26-0.45	Sparse	528.03	25.11	1594.52	75.83	201.98
0.46-0.59	Moderate	1291.42	61.42	230.86	10.98	-82.12
>0.6	Highly dense	172.95	8.23	0	0	-100

UHI effects

Developmental activities in any area will be associated with changes in LULC, resulting in loss of vegetative cover and increased surface temperatures. This subsequently triggers the genesis of UHIs. Figure 8 depicts the spatial distribution of UHI in Kottayam district for the year 1988 and 2020. The year 2020 was characterized by intense growth in UHI areas, where moderate, high and very high level

UHIs increased (Table 6). The occurrence of high UHI areas was more concentrated in the Kottayam taluk, followed by Meenachil and Changanassery, which showed good rate of development in the kottayam district indicating urban expansion. Intensity of UHI was associated with high LST areas. Rapid growth of industries and urbanisation coupled with loss of vegetation has proved to accelerate UHI formation.⁵⁷ In this context, Kottayam

district, being the prime rubber producer of the country provides large scale employment to people thus increasing settlement in the area. Reduction in natural vegetation, and increase in impervious surfaces like pavements, buildings, roofs etc., provides less shade and moisture, contributing to higher temperatures. Moreover, heat generated from human activities like movement of vehicles and industrial activities emit heat into urban environment, which can contribute to heat island effects.^{58,59} All these form a major reason for increase in high and very

high UHI classes from 1.34 % in 1988 to 40% in 2020, which is a tremendous increase. Conversely, areas under low and very low level UHIs decreased (Table 7) indicating urbanization process. Genesis of UHI associated with land cover change has been reported for Skopje, Macedonia.²⁵ Correlation analysis among LST and NDVI and NDBI suggested weaker UHI effects in green areas and strong UHI effects in the built-up areas which are similar to the results of the present study.

Table 5: Taluk wise spatial distribution of NDVI of Kottayam District during 1988 and 2020.

NDVI Categories	NDVI Classes	NDVI area in km ²									
		Vaikom		Meenachil		Kottayam		Kanjirappally		Changanassery	
		1988	2020	1988	2020	1988	2020	1988	2020	1988	2020
<0	No Vegetation	16.35	3.294	0.03	0.008	8.82	6.035	0.09	0.003	0.62	0.050
0-0.25	Very Low	31.84	83.172	11.87	73.976	27.50	77.585	3.38	12.9	9.73	20.1
0.26-0.45	Sparse	115.20	176.1	174.	552.3	117.	384.3	66.58	274.6	53.80	207.0
0.46-0.59	Moderate	103.28	8.171	500.	103.1	286.	29.8	246.	59.5	155.	30.1
>0.6	Highly dense	4.09	0	42.35	0	57.31	0	31.07	0.002	38.14	0

Table 6: Details of the UHI area during the study period for Kottayam Districts.

UHI Value	UHI Classes	1988		2020		% Difference (1988 and 2020)
		Area Km ²	Area %	Area Km ²	Area %	
< 0	No UHI	0	0	0	0	---
0 – 0.34	Very Low	500.34	23.80	35.95	1.71	-92.81
0.34 – 0.49	Low	1470.15	69.92	326.99	15.55	-77.76
0.49 – 0.56	Moderate	104.04	4.95	897.74	42.70	762.88
0.56 – 0.65	High	20.83	0.99	660.59	31.42	3071.34
>0.65	Very High	7.26	0.35	181.35	8.63	2397.93

URBAN HEAT ISLAND (UHI), 1988 AND 2020
KOTTAYAM DISTRICT, KERALA, INDIA

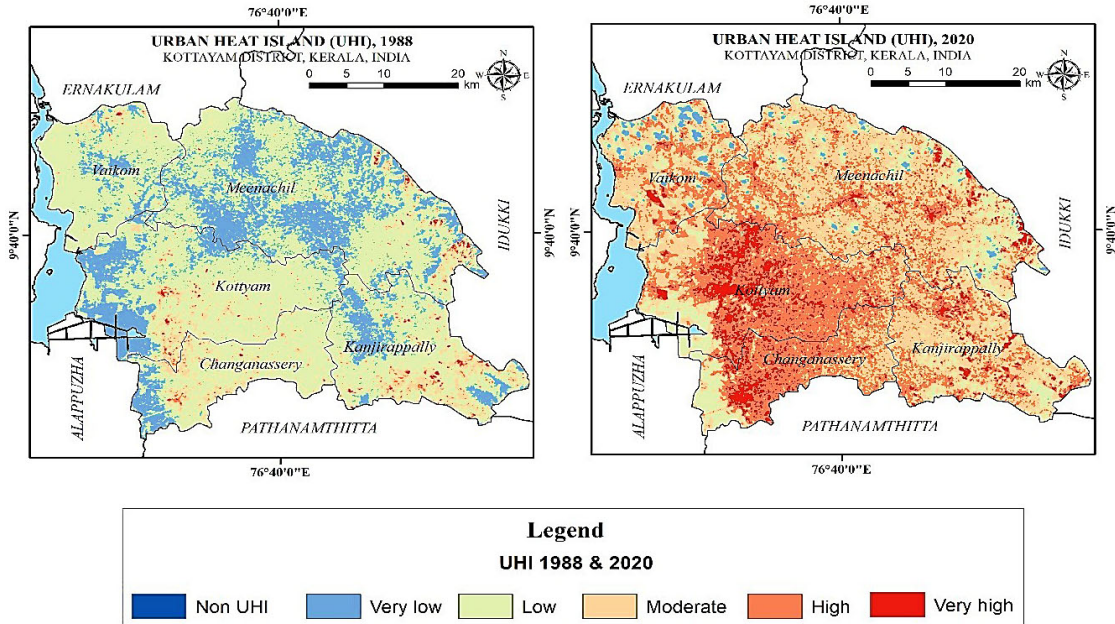


Fig. 8: Spatial distribution of UHI for the years 1988 and 2020

Table 7: Taluk wise spatial distribution of UHI of Kottayam District for the years 1988 and 2020.

UHI Catego-ries	UHI Clas-ses	UHI area in km ²									
		Vaikom		Meenachil		Kottayam		Kanjirappally		Changanassery	
		1988	2020	1988	2020	1988	2020	1988	2020	1988	2020
< 0	No UHI	0	0	0	0	0	0	0	0	0	0
0 – 0.34	Very Low	36.86	20.8	259.28	16.15	118.43	0.28	58.23	0.02	27.55	0
0.34 – 0.49	Low	227.69	53.44	446.63	145.25	349.83	51.47	243.29	54.05	202.73	32.39
0.49 – 0.56	Moderate	4.98	121.97	15.99	327.84	23.93	105.27	35.8	181.5	22.8	59.46
0.56 – 0.65	High	0.9	67.27	5.21	185.64	4.4	257.13	7.18	93.28	3.68	134.1
>0.65	Very High	0.33	7.28	2.37	24.6	1.24	83.69	2.67	18.3	0.65	31.43

Analysis of UTFVI

UTFVI was utilized to evaluate UHI impacts on ecological stability. UTFVI was classified as (Fig. 9) (i) excellent (ii) good (iii) normal (iv) bad (v) worse and (vi) worst based on ecological indexing. High

UTFVI values corresponds to high UHI intensity.⁶⁰ Both the study periods, 1988 and 2020 witnessed six levels of UTFVI (Table 8). However, when areas under excellent, normal and bad thermal comfort levels recorded a minimal decrease in

2020, areas under worst thermal comfort zone increased by 250% (Table 8), which was observed in the rapidly developing Meenachil and Kanjirappally taluks (Table 9). This was in good connection with LST, NDVI and UHI analysis of both the taluks. Such a remarkable increase in worst UTFVI class was also observed for Tianjin city, China, where increased UHI attributed to industrialisation and urbanisation⁴⁸ Analysis of UTFVI is considered as a

very important aspect since alterations in the UTFVI impose detrimental effects on native climatic conditions, indirect economic losses, decreased comfort, and increased mortality rates.⁶¹ Growing population density and urban climatic transitions, notably in terms of urban expansion and plant cover loss, have been shown to be important factors contributing to fluctuations in urban thermal conditions.⁶²⁻⁶⁵

Urban Thermal Field Variance Index (UTFVI), 1988 AND 2020 KOTTAYAM DISTRICT, KERALA, INDIA

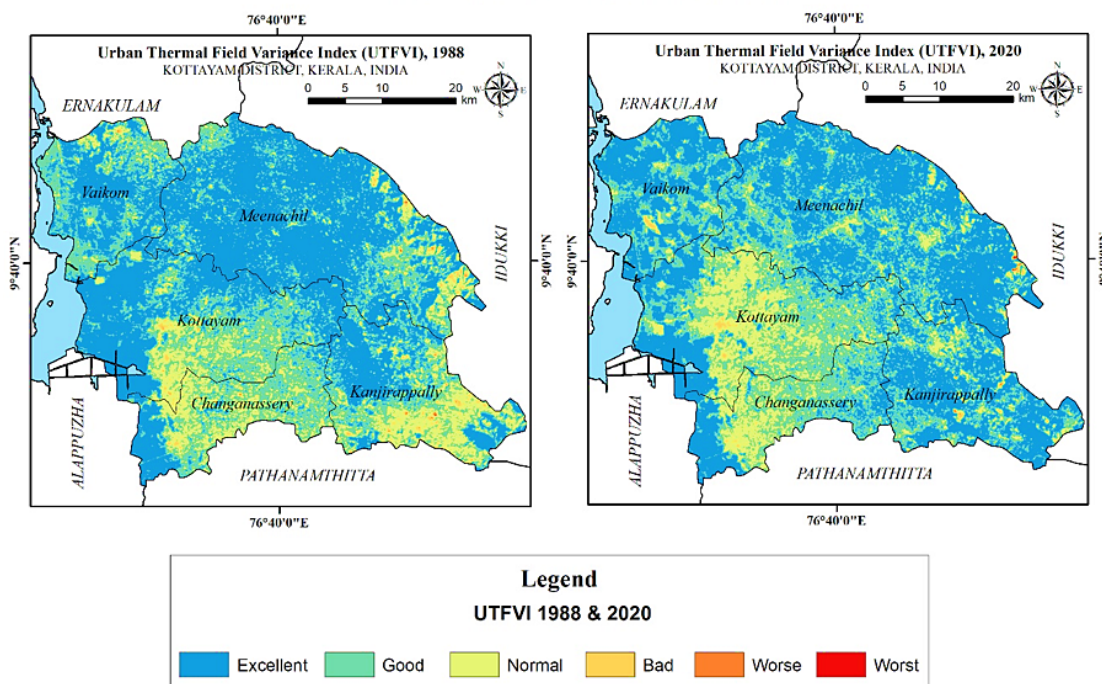


Fig. 9: Spatial distribution of UTFVI for the years 1988 and 2020

Table 8: Detailed Ecological Evaluation Index (EEI) of the study period for Kottayam Districts.

UTFVI	EEI	1988		2020		% Difference (1988 and 2020)
		Area Km2	Area %	Area Km2	Area %	
<0	Excellent	1076.36	51.191	1036.04	49.274	-3.75
0 – 0.05	Good	718.66	34.176	774.04	36.813	7.71
0.05 - 0.15	Normal	289.98	13.791	282.82	13.451	-2.47
0.15 - 0.25	Bad	16.57	0.788	8.95	0.426	-45.99
0.25 - 0.35	Worse	1.01	0.048	0.63	0.03	-37.62
>0.35	Worst	0.04	0.002	0.14	0.007	250

Table 9: Talukwise spatial distribution of EEI of Kottayam District for the years 1988 and 2020.

UTFVI Categories	EEI	LST area in km ²									
		Vaikom		Meenachil		Kottayam		Kanjirappally		Changanassery	
		1988	2020	1988	2020	1988	2020	1988	2020	1988	2020
<0	Excellent	135.25	173.04	511.49	456.72	249.73	128.56	124.92	205.4	54.96	72.32
0 – 0.05	Good	115.56	84.09	168.07	228.65	177.9	224.12	124.53	112.09	132.6	125.09
0.05 - 0.15	Normal	19.16	12.51	44.7	41.32	66.86	142.07	91.48	27.54	67.78	59.39
0.15 - 0.25	Bad	0.73	1.12	4.82	2.21	3.22	3.09	5.78	1.94	2.02	0.6
0.25 - 0.35	Worse	0.06	0	0.37	0.43	0.12	0.01	0.43	0.2	0.04	0
>0.35	Worst	0	0	0.02	0.14	0	0	0.02	0	0	0

Correlation between LST and NDVI

NDVI and LST are very sensitive to changes and variations in NDVI may initiate alterations in LST and vice versa. Fig. 10 and 11 confirms that NDVI shares a negative correlation with LST for the years 1988 and 2020 respectively [(R² = 0.5737 (1988) and 0.5199 (2020)], indicating that a dense vegetative cover lowered the surface temperature. High surface

temperatures were observed in areas of inactive or less vegetation, whereas low surface temperatures were associated with dense green vegetative areas, which prevents the earth’s surface from absorbing more radiation. Such negative correlation between LST and NDVI has been reported by several authors for various study regions like Wuhan, Lucknow, Vila Velha in Brazil, Skopje, Macedonia.^{24,49,66,25}

LST-NDVI Correlation Kottayam 1988

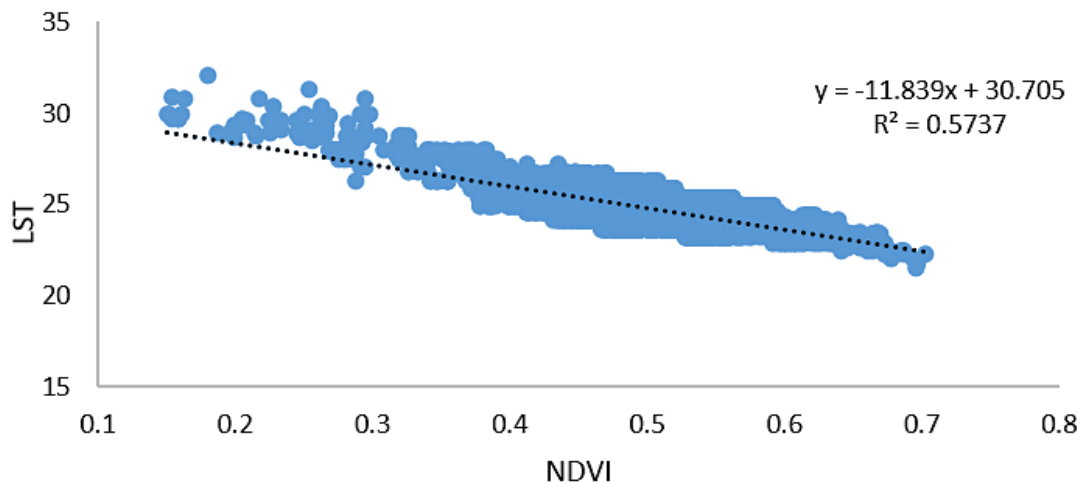


Fig. 10: LST-NDVI Correlation analysis

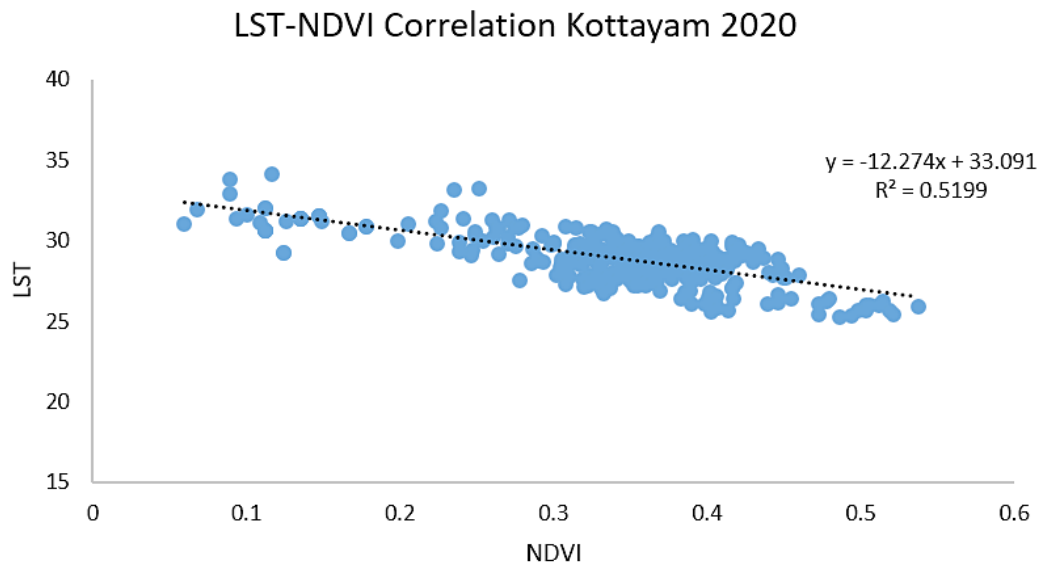


Fig. 11: LST-NDVI Correlation analysis, 2020

Conclusion

This study showed a negative relation between NDVI and LST and its impacts on UHI. The study shows that year by year, Kottayam district is experiencing an increase in temperature, which increases the UHI effect. Changes in LST and NDVI have occurred due to anthropogenic activities like urban expansion, which includes population rise, population migration, establishment of small and medium scale industries or enterprises, associated housing activities etc., resulting in altered energy balance, thereby triggering the formation of UHI. Formation of UHI is likely to cause adverse health, social economic and ecological impacts. Analysis of UHI in correlation with LST and vegetation index may be suggested as a useful tool for policy makers and planners in urban planning, as a strategy for sustaining ecological stability to improve the quality of lives. The study recommends that the local governing agencies should ensure to initiate actions increase areas under green cover in urban areas so as to mitigate UHI effects. The present

study employed Landsat data from specific years (1988 and 2020) and seasons (winter) which could limit the assessment of intermediate modifications that could have bypassed developments which may have influenced UHI dynamics. Moreover, integration of nighttime thermal data into such studies will offer more comprehensive insight into nocturnal UHI patterns.

Acknowledgement

The authors thank the Departments of Environmental Sciences, Bharathiar University, Coimbatore, and Environmental Science and management, Bharathidasan University, Thiruchirappalli, for their encouragement and facilities provided.

Funding

There is no funding or financial support for this research work.

Conflict of Interest

Authors declare that there is no any conflict of interest.

Reference

1. Kuang W, Liu A, Dou Y, Li G, Lu D. Examining the impacts of urbanization on surface radiation using Landsat imagery. *G/Science and Remote Sensing*. 2019; 56(3), 462-484. <https://doi.org/10.1080/15481603.2018.1508931>
2. Faqe Ibrahim, GR Urban land use land cover changes and their effect on land surface

- temperature: Case study using Dohuk City in the Kurdistan Region of Iraq. *Climate*. 2017; 5(1), 13. <https://doi.org/10.3390/cli5010013>
3. Hussain S, Mubeen M, Ahmad A, Majeed H, Qaisrani SA, Hammad HM, Amjad M, Ahmad I, Fahad S, Ahmad N, Nasim W. Assessment of land use/land cover changes and its effect on land surface temperature using remote sensing techniques in Southern Punjab, Pakistan. *Environmental Science and Pollution Research*. 2022; pp.1-17. <https://doi.org/10.1007/s11356-022-21650-8>
 4. Carpio M, González Á, González M, Verichev K. Influence of pavements on the urban heat island phenomenon: A scientific evolution analysis. *Energy and Buildings*. 2020; 226, 110379. <https://doi.org/10.1016/j.enbuild.2020.110379>
 5. Xiong Y, Huang S, Chen F, Ye H, Wang C, Zhu C. The impacts of rapid urbanization on the thermal environment: A remote sensing study of Guangzhou, South China. *Remote sensing*. 2012; 4(7), 2033-2056. <https://doi.org/10.3390/rs4072033>
 6. Streutker DR. Satellite-measured growth of the urban heat island of Houston, Texas. *Remote Sensing of Environment*. 2003; 85(3), 282-289. [https://doi.org/10.1016/S0034-4257\(03\)00007-5](https://doi.org/10.1016/S0034-4257(03)00007-5)
 7. Zhou B, Rybski D, Kropp JP. On the statistics of urban heat island intensity. *Geophysical research letters*. 2013; 40(20), 5486-5491. <https://doi.org/10.1002/2013GL057320>
 8. Siddique MA, Dongyun L, Li P, Rasool U, Khan TU, Farooqi TJA, Wang L, Fan B, Rasool MA. Assessment and simulation of land use and land cover change impacts on the land surface temperature of Chaoyang District in Beijing, China. *PeerJ*. 2020; 8, p.e9115.
 9. Lo CP, Quattrochi DA. Land-use and land-cover change, urban heat island phenomenon, and health implications: A remote sensing approach. *Photogrammetric engineering and remote sensing*. 2003; 69(9), 1053.
 10. Julien Y, Sobrino JA, Mattar C, Ruescas AB, Jimenez-Munoz JC, Soria G, Hidalgo V, Atitar M, Franch B, Cuenca J. Temporal analysis of normalized difference vegetation index (NDVI) and land surface temperature (LST) parameters to detect changes in the Iberian land cover between 1981 and 2001. *International Journal of Remote Sensing*. 2011; 32(7), pp.2057-2068. <https://doi.org/10.1080/01431161003762363>
 11. Mallick J, Kant Y, Bharath BD. Estimation of land surface temperature over Delhi using Landsat-7 ETM+. *J. Ind. Geophys. Union*. 2008; 12(3), 131-140.
 12. Dutta D, Rahman A, Paul SK, Kundu A. Impervious surface growth and its inter-relationship with vegetation cover and land surface temperature in peri-urban areas of Delhi. *Urban Climate*. 2021; 37, 100799. <https://doi.org/10.1016/j.uclim.2021.100799>
 13. Ramachandra TV, Uttam K. Land surface temperature with land cover dynamics: multi-resolution, spatio-temporal data analysis of Greater Bangalore. *International Journal of Geoinformatics*. 2009; 5(3), 44.
 14. Mathew A, Sarwesh P, Khandelwal S. Investigating the contrast diurnal relationship of land surface temperatures with various surface parameters represent vegetation, soil, water, and urbanization over Ahmedabad city in India. *Energy Nexus*. 2022; 5, 100044. <https://doi.org/10.1016/j.nexus.2022.100044>
 15. Vasanthawada SRS, Puppala H, Prasad PRC. Assessing impact of land-use changes on land surface temperature and modelling future scenarios of Surat, India. *International Journal of Environmental Science and Technology*. 2022; 1-14. <https://doi.org/10.1007/s13762-022-04385-4>
 16. Mukherjee F. Environmental Impacts of Urban Sprawl in Surat, Gujarat: An Examination Using Landsat Data. *Journal of the Indian Society of Remote Sensing*. 2022; 1-18. <https://doi.org/10.1007/s12524-022-01509-8>
 17. Gohain KJ, Mohammad P, Goswami A. Assessing the impact of land use land cover changes on land surface temperature over Pune city, India. *Quaternary International*. 2021; 575, 259-269. <https://doi.org/10.1016/j.quaint.2020.04.052>
 18. Siddiqui A, Kushwaha G, Nikam B, Srivastav SK, Shelar A, Kumar P. Analysing the day/night seasonal and annual changes and trends in land surface temperature and surface urban heat island intensity (SUHII) for Indian cities. *Sustainable Cities and Society*.

- 2021; 75, 103374. <https://doi.org/10.1016/j.scs.2021.103374>
19. Guha S, Govil H, Taloor AK, Gill N, Dey A. Land surface temperature and spectral indices: A seasonal study of Raipur City. *Geodesy and Geodynamics*. 2022; 13(1), 72-82. <https://doi.org/10.1016/j.geog.2021.05.002>
 20. Chandra S, Sharma D, Dubey SK. Linkage of urban expansion and land surface temperature using geospatial techniques for Jaipur City, India. *Arabian Journal of Geosciences*, 2018; 11, 1-12. <https://doi.org/10.1007/s12517-017-3357-6>
 21. Amirtham LR, Devadas MD, Perumal M. Mapping of micro-urban heat islands and land cover changes: a case in Chennai City, India. *The International Journal of Climate Change: Impacts and Responses*. 2009; 1(2), 71.
 22. Lo CP., Quattrochi DA. Land-use and land-cover change, urban heat island phenomenon, and health implications: A remote sensing approach. *Photogrammetric engineering and remote sensing*. 2003; 69(9), 1053.
 23. Weng Q, Lu D, Schubring J. Estimation of land surface temperature–vegetation abundance relationship for urban heat island studies. *Remote sensing of Environment*. 2004; 89(4), pp.467-483. <https://doi.org/10.1016/j.rse.2003.11.005>
 24. Zhang Y, Yiyun C, Qing D, Jiang P. Study on urban heat island effect based on normalized difference vegetated index: a case study of Wuhan City. *Procedia environmental sciences*. 2012; 13, 574-581. <https://doi.org/10.1016/j.proenv.2012.01.048>
 25. Kaplan G, Avdan U, Avdan ZY. March. Urban heat island analysis using the landsat 8 satellite data: A case study in Skopje, Macedonia. *In Proceedings*. 2018; 2(7), p. 358). <https://doi.org/10.3390/ecrs-2-05171>
 26. Tesfamariam S, Govindu V, Uncha A. Spatio-temporal analysis of urban heat island (UHI) and its effect on urban ecology: The case of Mekelle city, Northern Ethiopia. *Heliyon*. 2023; 9(2). <https://doi.org/10.1016/j.heliyon.2023.e13098>
 27. Bektaş Balçık, Filiz. Determining the impact of urban components on land surface temperature of Istanbul by using remote sensing indices. *Environmental monitoring and assessment* 2014; 186, 859-872.
 28. Grover A, Singh RB. Analysis of urban heat island (UHI) in relation to normalized difference vegetation index (NDVI): A comparative study of Delhi and Mumbai. *Environments*. 2015; 2(2), 125-138. <https://doi.org/10.3390/environments2020125>
 29. Macarof P, Statescu F. Comparasion of NDBI and NDVI as indicators of surface urban heat island effect in landsat 8 imagery: a case study of Iasi. *Present Environment and Sustainable Development*, (2), 2017; 141-150.
 30. Lu Y, Wu P, Zhu X, Jiang Y, Yin Z, Ma X. Comparison of surface urban heat island (SUHI) at landsat scale in Hefei, China: Diurnal, seasons and drivers. In 2018 Fifth International Workshop on Earth Observation and Remote Sensing Applications (EORSA) 2018; 1-4. IEEE.
 31. Xin J, Yang J, Wang LE, Jin C, Xiao X, Xia JC. Seasonal differences in the dominant factors of surface urban heat islands along the urban-rural gradient. *Frontiers in Environmental Science*. 2022; 1681.
 32. Aggarwal S, Misra M. October. Comparison of NDVI, NDBI as indicators of surface heat island effects for Bangalore and New Delhi: Case Study. In *Remote Sensing Technologies and Applications in Urban Environments III*. 2018; 10793, pp. 178-186. SPIE. <https://doi.org/10.1117/12.2325738>
 33. Mathew A, Khandelwal S, Kaul N. Investigating spatial and seasonal variations of urban heat island effect over Jaipur city and its relationship with vegetation, urbanization and elevation parameters. *Sustainable cities and society*. 2017; 35, 157-177. <https://doi.org/10.1016/j.scs.2017.07.013>
 34. Bora R, Bora AK. NDVI and NDMI indices based land use and land cover change analysis of Charaideu District, Assam, India. *Sustainability, Agri, Food and Environmental Research*, 2023; 11.
 35. Radhakrishnan S, Geetha P. Urban Sprawl Assessment Using Remote Sensing and GIS Techniques: A Case Study of Ernakulam District. In *Intelligent Sustainable Systems*. 2022; 293-307. Springer, Singapore.
 36. Mathew JC, Varghese A. Impact of Urbanization and Spatio-temporal Estimation of

- Land Surface Temperature in a Fast-growing Coastal Town in Kerala, Western Coast of Peninsular India. *Remote Sensing in Earth Systems Sciences*. 2022; 5(4), 207-229. <https://doi.org/10.1007/s41976-022-00075-4>
37. John J, Bindu G, Srimuruganandam B, Wadhwa A, Rajan P. Land use/land cover and land surface temperature analysis in Wayanad district, India, using satellite imagery. *Annals of GIS*. 2020; 26(4), 343-360. <https://doi.org/10.1080/19475683.2020.1733662>
 38. Prasad G, Ramesh MV. Spatio-temporal analysis of land use/land cover changes in an ecologically fragile area—Alappuzha District, Southern Kerala, India. *Natural Resources Research*. 2019; 28(1), 31-42. <https://doi.org/10.1007/s11053-018-9419-y>
 39. Landsat 8: Ihlen, V. 2019. Landsat 8 data users handbook. *US Geological Survey: Sioux Falls, SD, USA*, 55.
 40. Barsi JA, Schott JR, Hook SJ, Raqueno NG, Markham BL, Radocinski RG. Landsat-8 thermal infrared sensor (TIRS) vicarious radiometric calibration. *Remote Sensing*. 2014; 6(11), pp.11607-11626. <https://doi.org/10.3390/rs6111607>
 41. Landsat 5: Landsat 7 (L7) Data Users Handbook. Available online: https://prd-wret.s3-us-west-2.amazonaws.com/assets/palladium/production/atoms/files/LSDS-1927_L7_Data_Users_Handbook-v2.pdf (accessed on 5 December 2019).
 42. Chander G, Markham B. Revised Landsat-5 TM Radiometric Calibration Procedures and Postcalibration Dynamic Ranges. *IEEE Transactions on Geoscience and Remote Sensing*. 2003; 41:2674–2677. <https://doi.org/10.1109/TGRS.2003.818464>
 43. Snyder WC, Wan Z, Zhang Y, Feng YZ. Classification-based emissivity for land surface temperature measurement from space. *International Journal of Remote Sensing*. 1998; 19, 2753–2774. <https://doi.org/10.1080/014311698214497>
 44. Artis DA, Carnahan WH. Survey of emissivity variability in thermography of urban areas. *Remote Sensing of Environment*. 1982; 12:313–329. [https://doi.org/10.1016/0034-4257\(82\)90043-8](https://doi.org/10.1016/0034-4257(82)90043-8)
 45. Dissanayake DMSLB, Morimoto T, Ranagalage M, Murayama Y. 2019. Land-use/land-cover changes and their impact on surface urban heat islands: Case study of Kandy City, Sri Lanka. *Climate* 7. <https://doi.org/10.3390/cli7080099>
 46. Tucker CJ. 1979. Red and photographic infrared linear combinations for monitoring vegetation. *Remote Sensing of Environment* 8:127–150. [https://doi.org/10.1016/0034-4257\(79\)90013-0](https://doi.org/10.1016/0034-4257(79)90013-0)
 47. Townshend JR, Justice CO. Analysis of the dynamics of African vegetation using the normalized difference vegetation index. *International journal of remote sensing*. 1986; 7(11), 1435-1445. <https://doi.org/10.1080/01431168608948946>
 48. Ullah N, Siddique MA, Ding M, Grigoryan S, Zhang T, Hu Y. Spatiotemporal Impact of Urbanization on Urban Heat Island and Urban Thermal Field Variance Index of Tianjin City, China. *Buildings*. 2022; 12(4), 399. <https://doi.org/10.3390/buildings12040399>
 49. Singh P, Kikon N, Verma P. Impact of land use change and urbanization on urban heat island in Lucknow city, Central India. A remote sensing based estimate. *Sustainable cities and society*. 2017; 32, 100-114. <https://doi.org/10.1016/j.scs.2017.02.018>
 50. Guo, L.; Liu, R.; Men, C.; Wang, Q.; Miao, Y.; Zhang, Y. Quantifying and simulating landscape composition and pattern impacts on land surface temperature: A decadal study of the rapidly urbanizing city of Beijing, China. *Sci. Total Environ*. 2019; 654, 430–440.
 51. Govt. of India, MSME: <https://dcmsme.gov.in/old/dips/Dt%20%20profile-%20KOTTAYAM-WORKING.pdf>
 52. Sayão VM, dos Santos NV, de Sousa Mendes W, Marques KP, Safanelli JL, Poppiel RR, Demattê JA. Land use/land cover changes and bare soil surface temperature monitoring in southeast Brazil. *Geoderma Regional*. 2020; 22:e00313.
 53. Chattopadhyay S. Environmental consequences of rubber plantations in Kerala. 2021.
 54. Ling Z, Shi Z, Gu S, Wang T, Zhu W, Feng, G. Impact of Climate Change and Rubber (Hevea brasiliensis) Plantation Expansion on Reference Evapotranspiration in Xishuang-

- banna, Southwest China. *Frontiers in Plant Science*. 2022; 13, 159. <https://doi.org/10.3389/fpls.2022.830519>
55. Ramkrishnan R, Ramachandra TV. Four decades of forest loss: Droughts in Kerala (Poster). In *Lake 2016: Conference on Conservation and Sustainable Management of Ecologically Sensitive Regions in Western Ghats, 10th Biennial Lake Conference: Wetlands for Our Future*.
56. Yirsaw E, Wu W, Shi X, Temesgen H, Bekele B. Land use/land cover change modeling and the prediction of subsequent changes in ecosystem service values in a coastal area of China, the Su-Xi-Chang Region. *Sustainability*. 2017; 9(7), 1204. <https://doi.org/10.3390/su9071204>
57. Giannopoulou K, I Livada, M Santamouris, M Saliari, M Assimakopoulos, and YG Caouris. On the characteristics of the summer urban heat island in Athens, Greece. *Sustainable Cities and Society* 1, no. 1. 2011; 16-28.
58. Chen W, Zhang Y, Pengwang C, Gao W, Evaluation of urbanization dynamics and its impacts on surface heat islands: A case study of Beijing, China. *Remote Sens*. 2017, 9, 453.
59. Thanh Hoan N, Liou YA, Nguyen KA, Sharma RC, Tran, DP, Liou CL, Cham DD, Assessing the effects of land-use types in surface urban heat islands for developing comfortable living in Hanoi City. *Remote Sens*. 2018; 10, 1965
60. Kusumawardani KP, Hidayati IN. November. Analysis of urban heat island and urban ecological quality based on remote sensing imagery transformation in Semarang city. In *IOP Conference Series: Earth and Environmental Science*. 2022; Vol. 1089, No. 1, p. 012037. IOP Publishing. 10.1088/1755-1315/1089/1/012037
61. Sejati AW, Buchori I, Rudiarto I. February. The impact of urbanization to forest degradation in Metropolitan Semarang: A preliminary study. In *IOP conference series: Earth and environmental science*. 2018; Vol. 123, No. 1, p. 012011. IOP Publishing. 10.1088/1755-1315/123/1/012011
62. Amir Siddique M, Wang Y, Xu N, Ullah N, Zeng P. The Spatiotemporal Implications of Urbanization for Urban Heat Islands in Beijing: A Predictive Approach Based on CA-Markov Modeling (2004–2050). *Remote Sens*. 2021; 13, 4697
63. Li J, Zhang C, Zheng X, Chen Y. Temporal-Spatial Analysis of the Warming Effect of Different Cultivated Land Urbanization of Metropolitan Area in China. *Sci. Rep.* 2020; 10, 2760.
64. Xu J, Zhao Y, Sun C, Liang H, Yang J, Zhong K, Li Y, Liu X. Exploring the Variation Trend of Urban Expansion, Land Surface Temperature, and Ecological Quality and Their Interrelationships in Guangzhou, China, from 1987 to 2019. *Remote Sens*. 2021; 13, 1019.
65. Rouibah K, Belabbas M. Applying Multi-Index approach from Sentinel-2 Imagery to Extract Urban Area in dry season (Semi-Arid Land in North East Algeria). *Rev. Teledetección* 2020; 56, 89–101.
66. Dos Santos AR., de Oliveira FS, da Silva A G, Gleriani, JM, Gonçalves W, Moreira GL, Silva FG, Branco ERF, Moura MM, da Silva RG, Juvanhol RS. Spatial and temporal distribution of urban heat islands. *Science of the Total Environment*. 2017; 605, pp.946-956.